

Poly[(2,2',5',2''-tetramethoxy-*p*-terphenyl-5,5''-ylene)propylene]: Synthesis and physical properties of a novel amorphous regularly segmented conjugated polymer

Pablo G. Del Rosso ^a, Marcela F. Almassio ^a, Pedro Aramendia ^b,
Silvia S. Antollini ^c, Raúl O. Garay ^{a,*}

^a Instituto de Investigaciones en Química Orgánica, Universidad Nacional del Sur, Avenida Alem 1253, 8000-Bahía Blanca, Argentina

^b INQUIMAE and Departamento de Química Inorgánica, Analítica y Química Física, FCEN, Universidad de Buenos Aires, Pabellón 2, Ciudad Universitaria, C1428EHA Buenos Aires, Argentina

^c Instituto de Investigaciones Bioquímicas de Bahía Blanca, Camino La Carrindanga Km 7 – C.C. 857, 8000 Bahía Blanca, Argentina

Received 17 October 2006; received in revised form 12 March 2007; accepted 13 March 2007

Available online 20 March 2007

Abstract

A new regularly segmented conjugated polymer with methoxy-substituted *p*-terphenylene units tethered by their meta positions along the polymer main chain was synthesised using the Suzuki cross-coupling reaction. The small size of the connector and lack of long lateral chains lead to a high density of rigid electrooptically active moieties in the structure. However, this molecular architecture produces a very soluble and amorphous polymer with relatively high T_g . The optical properties of samples with different degrees of polymerisation were investigated using UV–visible absorption, steady state and time-resolved photoluminescence emission spectroscopies. Their absorption and emission properties are rather insensitive to Mn after reaching a modest DP, to the aggregation state, either solution or neat film, and to annealing. The contorted polymer chain forms a very stable morphology and substantially hinders interactions between chromophores, thus diminishing the formation of aggregated species that are commonly observed in other electrooptically active polymers.

© 2007 Elsevier Ltd. All rights reserved.

Keywords: Segmented conjugated polymer; Amorphous; Luminescent; Synthesis

1. Introduction

Control over materials morphology is an important matter in materials science and functional applications [1]. Thus, a number of recent studies

have analysed the role of morphology in the final properties of conjugated polymers [2]. Conjugated polymers can exist in a large number of morphological organizations at the molecular and nanoscopic levels. These organizations spring from the interrelation between two of the intrinsic properties of these polymers. While the rigidity of their aromatic segments promotes crystalline ordering or aggregate formation, the structural flexibility, conferred

* Corresponding author. Tel.: +54 291 4595101; fax: +54 291 4595679.

E-mail address: rgaray@criba.edu.ar (R.O. Garay).

either conformationally or by saturated groups placed in the main chain, generates highly disordered areas [3]. On the other hand, amorphous molecular glasses is a new materials class characterized by their high density of active units, good processability, transparency and homogeneous properties [4]. Amorphous molecular materials represent an approach based on the concept that the non-planarity of organic molecules can suppress molecular packing to solve the inconveniences that emerge from the crystallinity, extensive aggregation and morphological heterogeneity of conjugated polymers. However, polymeric systems have traditionally been associated with highly stable amorphous states under thermal stress, with mechanical properties that cannot be paralleled by molecular systems and with much lower diffusion mobilities in multilayer devices than those showed by molecular materials.

In particular, there has been much interest regarding segmented conjugated polymers in relation to the application of their electroluminescent properties, especially in the blue region, in organic light-emitting diodes. Regrettably, the rigid aromatic units have a strong tendency to form interchain species such as aggregates or excimers; especially when the spacers consist of flexible chains which provide the conformational freedom needed to adopt more ordered structures in the solid state [5,6]. In comparison to emission from non-interacting chromophores these ordered structures have red-shifted emission contributions and lower photoluminescent efficiencies [7].

However, if the spacer is reduced to a single saturated carbon atom the polymer main chain is forced to adopt bent conformations that would likely lead to the formation of amorphous phases. A small number of photoactive polymeric materials that have norbornylene [8] or fluorenylene [9] spacers have been reported but the influence of their morphology on the electrooptical properties was not explored. The molecular architecture of all reported segmented conjugated polymers of this kind comprise linear aromatic units linked by their para positions to the saturated spacer and long lateral chains in order to impart processability to them. But along with the improvement of the polymer solubility the lateral chains dilute the active moieties in the polymer structure. However, adequate design could render amorphous polymeric materials that incorporate rigid electrooptically active units with no dilution of active chromophores and whose mor-

phology and processability would be determined by the main chain configuration.

In this article we report the synthesis and characterization of a polymer composed of methoxy-substituted *p*-terphenylene units tethered by their meta positions along the polymer main chain and separated by isopropylene spacers. We study how the chain configuration and molecular weight of the polymer influenced its processability, morphology and optical properties. Its optical properties were investigated using UV–visible absorption and both steady state and time-resolved photoluminescence emission (PL) spectroscopies.

2. Experimental

2.1. Materials

Bisphenol A (BPA) (Aldrich) and *p*-dimethoxybenzene (Aldrich) were recrystallised from ethanol prior to use. Tetrakis(triphenylphosphine)palladium(0) was prepared as described in the literature [10] and then was washed with ethyl ether and EtOH according to an established procedure [11]. Toluene was purified by distillation and water by bidistillation. THF was purified by distillation from Na/benzophenone. Reagents and solvents were purchased from Aldrich and used without further purification unless otherwise specified.

2.2. Monomer synthesis

2.2.1. 2,2-bis-(2-bromo-4-methoxyphenyl)propane (**1**)

This compound was obtained in two steps. First, a well-stirred mixture of BPA (2.30 g, 10.0 mmol) and K_2CO_3 (3.50 g, 25.0 mmol) in acetone (12 mL) was heated under reflux for 1 h, and then methyl iodide (4.00 g, 28.0 mmol) was added. The suspension was warmed at 30–35 °C for 3 days. Water (20 mL) was then added, the mixture stirred for 10 min at room temperature and extracted with $CHCl_3$ (three times 10 mL). The combined organic layers were washed with water, aqueous NaOH, aqueous HCl and water, dried with Na_2SO_4 and the solvent was removed under reduced pressure. 2,2-bis-(4-methoxyphenyl)propane was obtained as a dense liquid after purification by column chromatography on silica gel using hexane/ CH_2Cl_2 as eluent. Yield: 2.57 g (79%). 1H NMR ($CDCl_3$): δ = 7.14 (d, 2H, J_0 8.77), 6.79 (d, 2H, J_0 8.77), 3.76 (s, 3H), 1.63 (s, 3H). ^{13}C NMR ($CDCl_3$): δ = 157.8, 143.6, 128.2, 113.7, 55.6, 42.1, 31.5.

Then, Br₂ (2.74 g, 17.2 mmol) was added dropwise over a period of 40 min to a solution of 2,2-bis-(4-methoxyphenyl)propane (2.00 g, 7.8 mmol) in CH₂-Cl₂ at 0 °C (6 mL). The mixture was stirred for 5 h followed by the addition of a 10% aqueous NaOH solution (15 mL). The mixture was then extracted with CH₂Cl₂ (three times 5 mL), the organic layer was dried with Na₂SO₄ and the solvent was removed under reduced pressure. Compound **2** was obtained as a very dense liquid after purification by column chromatography on silica gel using hexane/CH₂Cl₂ as eluent. Yield: 2.77 g (86%). ¹H NMR (CDCl₃): δ = 7.39 (d, 1H, *J_m* 2.29), 7.07 (dd, 1H, *J_m* 2.29, *J_o* 8.58), 6.79 (d, 1H, *J_o* 8.58), 3.87 (s, 3H), 1.61 (s, 3H). ¹³C NMR (CDCl₃): δ = 154.3, 144.4, 131.3, 127.2, 111.9, 111.7, 56.6, 42.1, 31.3. (C₁₇H₁₈Br₂O₂) (414.1): Calcd. C, 49.30; H, 4.38; Found: C, 49.18; H, 4.32.

2.2.2. 2,5-dimethoxyphenyl-1,4-bis(trimethyleneboronate) (**3**)

First, 2,5-dimethoxy-1,4-phenylenediboronic acid (**2**) was prepared from *p*-dimethoxybenzene by dibromination and dilithiation followed by addition of triisopropyl borate as described in the literature [12]. After that, a mixture of the diboronic acid (5.0 mmol, 1.14 g), 1,3-dihydroxypropane (0.89 g, 11.8 mmol) and toluene (54 mL) was heated under reflux for 2.5 h. Water formed during the reaction was removed by azeotropic distillation and collected in a Dean–Stark trap. The toluene was then removed under reduced pressure. The resulting solid was dissolved in CHCl₃ (50 mL), dried with SO₄Mg and the solvent was evaporated. The product was purified by recrystallization from toluene/hexane (7:5) to give white crystals of **3**. Yield: 1.21 g (78%); m.p. 189 °C. ¹H NMR (CDCl₃): δ = 7.16 (s, 1H), 4.17 (t, 2H, *J* 5.53), 3.82 (s, 3H), 2.03 (q, 4H, *J* 5.53). ¹³C NMR (CDCl₃): δ = 158.1, 118.6, 62.6, 56.9. (C₁₄H₂₀B₂O₆) (305.9): Calcd. C, 54.96; H, 6.59; Found: C, 54.82; H, 6.51.

2.2.3. Poly(2,2',5',2''-tetramethoxy-*p*-terphenyl-5,5''-ylene)propylene (**4a–d**)

The general procedure used for the synthesis of polymers **4a–d** is described in detail for **4d**. A 50 mL Schlenk tube was charged with Pd(PPh₃)₄ (0.44 g, 0.38 mmol), **3** (0.83 g, 2.00 mmol), Na₂CO₃ (2.82 g, 26.6 mmol) and comonomer **6** (0.623 g, 2.00 mmol) and the mixture was kept under Ar atmosphere. Dry THF (13.3 mL) and water (13.3 mL) were added via a syringe. The mixture was heated at 80 °C for 7

days. The reaction mixture was poured into methanol (30 mL). The precipitate was collected by filtration and dissolved in CHCl₃ (4 mL). The solution was filtered and poured into methanol (30 mL). The precipitate was collected by filtration and dried under vacuum (0.24 g; 51%). ¹H NMR (CDCl₃): δ = 7.27 (d, 1H⁹, *J_m* 2.28), 7.20 (dd, 1H⁵, *J_o* 8.60, *J_m* 2.28), 6.87 (s, 1H¹²), 6.86 (d, 1H⁶, *J_o* 8.60), 3.76 (s, 3H³), 3.63 (s, 3H⁴), 1.7 (s, 3H¹). ¹³C NMR (CDCl₃): δ = 154.8 (C⁷), 150.9 (C^{11,12'}), 142.6 (C⁴), 130.6 (C^{8,9}), 127.8 (C^{10,13}), 126.8 (C⁵), 115.9 (C⁶), 110.5 (C^{11',12}), 56.6 (C¹⁴), 55.7 (C³), 41.8 (C²), 31.2 (C¹). (C₂₅H₂₆O₄)_{*n*} (390.5)_{*n*}: Calcd. C, 76.90; H, 6.71; Found: C, 76.48; H, 6.52.

2.3. Measurements

Melting points reported are not corrected. Elemental analyses were made at INQUIMAE, UBA. ¹H NMR and ¹³C NMR spectra were recorded on a Bruker ARX300 spectrometer on samples dissolved in CDCl₃; all signals assigned with the help of polarisation transfer DEPT135 ¹³C and 2D(¹H–¹³C) correlation NMR experiments. Gel permeation chromatography analyses were carried out on THF solutions at room temperature using a Waters model 600 equipped with a Waters 2487 UV detector set at 254 nm. Calibration of the instrument was done using polystyrene standards. Thermal analysis was carried out on a Perkin Elmer DSC7 under nitrogen flow. The scan rate was 10 °C/min. The thermal behaviour was observed on an optical polarizing microscope (Leitz, Model Ortolux) equipped with a hot stage (Mettler).

UV/vis spectra were obtained using a UV–visible GBC Cindra 20 spectrometer. The absorption measurements were done either on dilute samples (less than 0.01 g/mL) or on thin films cast on quartz plates, which were placed at a 30° angle with respect to the incident beam. Steady-state fluorescence spectra were obtained using a SML AMINCO 4800 spectrofluorimeter at 25 °C. The time resolved measurements were obtained using a TimeMaster PT1 spectrofluorimeter with band pass-filters (excitation, UG1; emission, WG375) at 25 °C. The emission measurements were carried out on dilute samples (less than 0.02 mg/mL) using a 1 cm cuvette and keeping the optical densities below 0.1 to minimize aggregation and reduce artefacts introduced by self-absorption in fluorescence. Front-face measurements were made on concentrated samples (c.a. 1–5 mg/mL) using a 1 mm cuvette or on thin films cast on

quartz plates. Both the illuminated surface of the 1 mm cuvette and the quartz plates were oriented 30° relative to the incident beam. Film specimens were drop-cast from a CHCl₃ solution or a CHCl₃ solution of 1% w/w of **4** in PMMA (Aldrich, MW 120,000) on quartz substrates and dried at room temperature.

2.4. Molecular modelling

Molecular modelling of the dimer was carried out at the semiempirical level using the PM3 MO program implemented in the suite of programs Hyperchem (Version 7.0, Hypercube Inc.). Modelling was assumed to be carried out in the gas phase at 0 K. Minimisation operations were performed using the conjugate gradient method and halted by setting the gradient option at 0.01 kcal/mol. The lowest potential energy conformations were found by minimisation of the energy function in conjunction with a conformational search around the single bond that links the aromatic ring to the isopropylene spacer using the MM+ program.

3. Results and discussion

Poly(*p*-arylene alkylene)s is not a well-known polymer class [13] though one of their families, the poly(*p*-xylylene)s, have attracted much attention [14,15] and another, the poly(*p*-biphenylene methylene)s, is being considered as a candidate for bistable organic memory devices [16]. In these polymers, as the size of the alkylene moiety dwindles, or the size of the aromatic moiety increases, processability is severely reduced [13]. Indeed, poly(*p*-arylene alkylene)s without side chains have inherently limited solubilities. Besides, the substitution pattern in the aromatic ring is of importance in this matter, thus poly(*m*-phenylene methylene) of DP = 24 is soluble in THF [17]. But poly(*p*-biphenylene methylene)s are sparingly soluble in common organic solvents [16]. However electrooptical properties of interest

can only be achieved with larger aromatic units. Therefore, our target polymer was designed with tetra methoxy-substituted *p*-terphenylene units tethered to an isopropylidene unit by their meta-positions. We reason that the presence of methoxy groups should enhance solubility, by virtue of their interactions with solvents, and the meta links on conformational grounds. Thus, a phenyl ring flip around the single bond that links the rings to the isopropylene spacer in a para-linked polymer does not alter significantly the overall main chain conformation. In contrast, the same rotations in a meta-linked polymer switch between very different conformations, notably increasing the degrees of freedom of the polymer main chain. For instance, the minimised extended conformation of a dimer of **4** and its bent conformation, which was generated from the extended one by a ring flip and then minimised, see Fig. 1, have close relative minima potential energy values, $H_{\text{ext}} - H_{\text{bent}} = 0.07$ kcal/mol. Thus, modelling indicates that bent and extended conformations will contribute significantly to the total conformational population at room temperature; rendering contorted chains with little ability to order themselves in concentrated solutions or during and after solidification.

A summary of the synthesis of the monomers and polymers is shown in Scheme 1. Dibromide **2** was prepared in good yields from BPA by methylation followed by dibromination at low temperature in order to avoid polybromination. Diboronic acid **5** was prepared as described in the literature from the dibromide by treatment of its dilithium salt with isopropyl borate followed by acidic hydrolysis. Diboronate ester **3** was synthesised from the boronic acid by azeotropic esterification with 1,3-propanediol. Polymers **4a–d** were synthesised by Suzuki cross-coupling reactions between the dibromide **1** and either the diboronic acid **2** or the ester **3** in yields of 43–68% after reprecipitation. The polymers did not precipitate in the reaction mixture and best results were obtained with freshly prepared

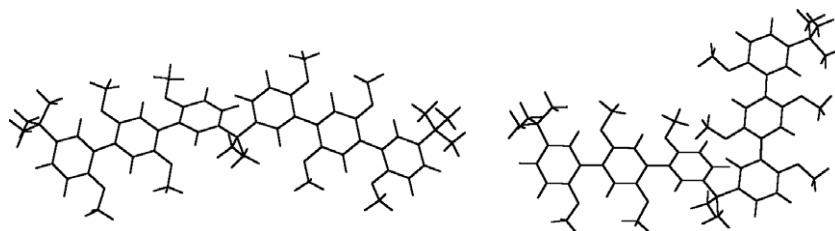
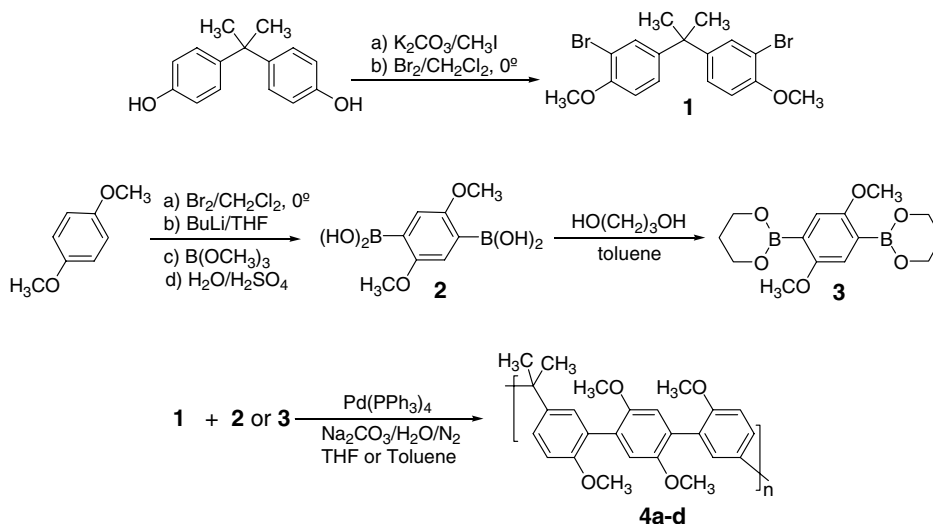


Fig. 1. PM3 molecular model of extended and bent conformations of a dimer of **4**.

Scheme 1. Synthesis of monomers and polymers **4a-d**.

$(\text{PPh}_3)_4\text{Pd}(0)$ that was then washed with ethyl ether and EtOH. The use 1,3-propanediol ester **3** (see entries 3 and 4 in Table 1) in place of boronic acid **2** (entries 1 and 2) was also beneficial as well as the use of THF (entries 2 and 4) as solvent instead of toluene.

The gel permeation analysis (Table 1) showed that **4a-b** were oligomeric materials with a rather narrow distribution due to the reprecipitation from MeOH, that **4b-d** showed monomodal distributions and that a reasonable number-average molecular weight was achieved for **4d**. It is worth mentioning that light scattering techniques have indicated that GPC measurements using polystyrene standards underestimate 1.5 or 1.8 times the real average molecular weights in this class of polymers [16,18]. As expected, the ^1H and ^{13}C NMR spectra showed that **4a** and **4b** have higher structural heterogeneity than **4c** and **4d** due to the chain ends and that **4d** has

a well-defined structure. Fig. 2 shows the ^1H spectrum obtained from polymer **4d**. Polymers have good solubility in common organic solvents. Particularly, its solubility in CHCl_3 is remarkable and we were able to prepare 50 wt.% CHCl_3 solutions of **4d** from which brittle fibres can be easily pulled out. Films drop-cast on quartz plates and dried under vacuum gave smooth films suitable for optical measurements. When concentrated solutions were used, the films could also be pulled out from the glass substrate to form homogeneous transparent freestanding films though their average molecular weight is not very high.

The thermal properties were investigated using DSC and polarized optical microscopy (POM). DSC was performed at a temperature range between 50 and 250°C . **4a-d** are amorphous in nature; their DSC traces showed only distinct glass transitions

Table 1
Physical properties of **4a-d**

	M_n/M_w^a	PDI	DP_n	T_g^b	$\lambda_{\text{Abs,max}}^c$ A/B ^c	$\lambda_{\text{PL,max}}^d$ A/B ^d	hwhm A/B ^e	SS ^f
4a	1100/1400	1.25	3	104	304/304	365, 379/363, 398, 452, 516	57/146	94
4b	1750/2200	1.25	5	105	303/302	363, 379/363, 377	58/71	61
4c	3200/5050	1.58	8	141	304/304	363, 377/363, 379	57/67	79
4d	7100/10,700	1.51	18	161	304/304	363, 377/363, 379	58/64	75

^a In g mol^{-1} determined by GPC (THF, against polystyrene standards).

^b In $^\circ\text{C}$, glass transition temperatures determined by DSC at scan rates of $10^\circ\text{C}/\text{min}$.

^c Absorption maxima (in nm) measured from dilute CHCl_3 solutions (A) and thin films drop-casted from CHCl_3 solutions (B).

^d Emission maxima (in nm) measured from dilute CHCl_3 solutions (A) and thin films drop-casted from CHCl_3 solutions (B). Bold data indicate the major peaks.

^e Full width at half-maximum of the fluorescence bands (in nm) in solutions (A) and films (B).

^f Stokes shifts in films ($\lambda_{\text{PL,max}}(0-1 \text{ band}) - \lambda_{\text{Abs,max}}$, in nm). For **4b**, $\lambda_{\text{PL,max}}(0-0 \text{ band})$.

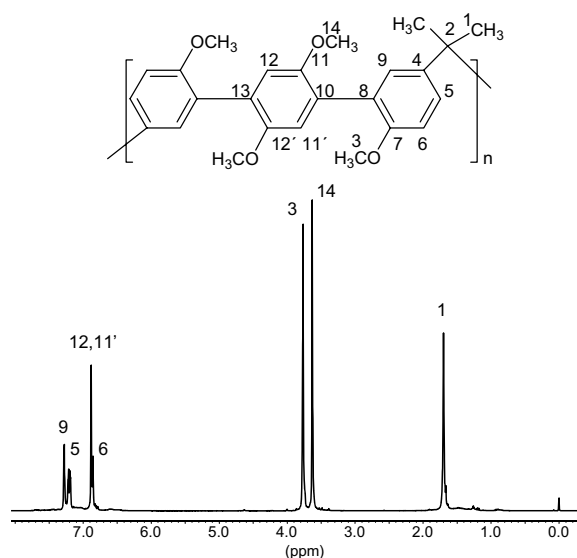


Fig. 2. ^1H NMR spectrum of **4d** in CDCl_3 .

with a noticeable molecular weight effect and no melting transitions were found upon heating beyond the glass transition temperature. Besides, no birefringence was detected by POM observations in the same temperature range. The rather high T_g temperature showed by **4d** reflects the polymer chain rigidity and absence of conformationally rich aliphatic side chains (Fig. 3).

The optical properties of **4a–d** were investigated using UV–visible absorption and steady state and time-resolved photoluminescence emission (PL). The absorption and PL spectra of dilute chloroformic solutions and film spectra of **4a**, **4b** and **4d** are shown in Fig. 4 and the wavelength maxima recorded in different conditions are summarised in Table 1.

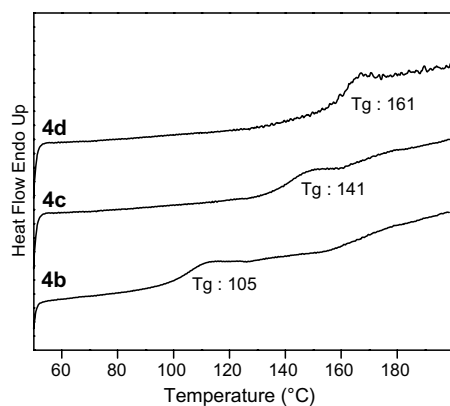


Fig. 3. DSC traces of **4b–d**.

The solution absorption spectra in chloroform of **4a–d**, as well as their film absorption spectra, are identical. In principle, provided that the synthetic procedure does not introduce structural defects, independence of absorption properties on the degree of polymerisation is expected in highly dilute solutions in a good solvent for a series of regularly segmented conjugated polymers that have the same structurally well-defined chromophores. Therefore, the observed similarity of the absorption spectra argues for a regular structure of **4a–d**, the weight of terminal groups relative to the macromolecule total mass being the main source of structural differences among the members of this series; variation which bears no significance in the case of photon absorption in dilute solutions. It is well known that the room temperature absorption spectrum of *p*-terphenyl lacks vibrational structure while its emission spectrum shows vibronic bands [19]. Such absence of mirror symmetry between absorption and fluorescence is assigned to the planarization of the first excited state structure as compared to the non-planar ground state that result in moderate Stokes shifts of 47 nm and 62 nm for the *p*-terphenyl 0–0 and 0–1 emission vibronic bands. The tetramethoxy-substituted *p*-terphenyl chromophore of **4a–d** shows a similar pattern. Its unstructured absorption band is distinctive of chromophores having a non-planar geometrical structure with relatively low torsional barriers between conformations around C–C single bonds that present a distribution of ground states with different ring-torsion angles such as α,α' -oligothiophenes [20], *p,p'*-oligophenylenes [21] or oligophenylenevinyls [22]. However, compared to *p*-terphenyl its Stokes shifts are slightly larger, 59 nm and 75 nm. Since the methoxy substitution red-shifts the absorption and emission bands in **4a–d** by 28 nm and 40 nm respectively, it follows that the electron donor properties of the methoxy groups improve electron delocalisation along the chromophore while their larger steric demands do not hinder planarization, being their influence larger in the excited state. As a matter of fact it has been demonstrated for oligothiophenes that methoxy substitution favours planarization of the excited states [23]. In addition, each sample shows no considerable differences between their solution and film absorption spectra indicating that in the amorphous state the weight of the fraction of more planar rotamers is not appreciably increased in the conformational population of chromophores by ground-state interactions between chains. In contrast, the absorption maxima

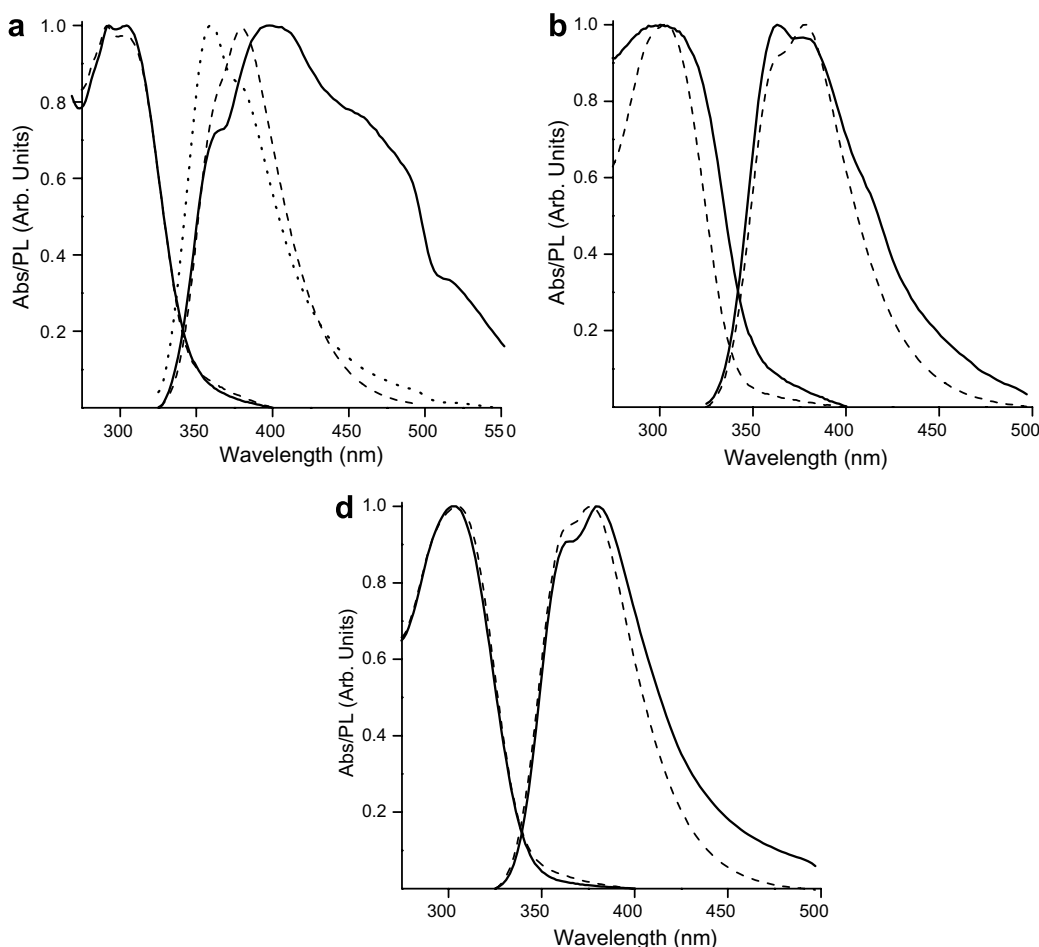


Fig. 4. Normalized absorption and emission spectra of CHCl_3 solutions (dashed curves) and films (solid curves) of **4a**, **4b** and **4d**. The emission spectrum of a PMMA film containing 1% w/w of **4a** is also included (dotted curve). The PL spectra were obtained by excitation at 310 nm.

of fully conjugated polymers usually present a red shift in the solid film as compared to the dilute solution [24], which has been explained as an effect of interchain π -stacking [25]. As mentioned before, the individual polymer chains have a contorted open topology. Therefore, vicinal chains likely interpenetrate each other in the solid state placing the nearby terphenylene chromophores in close contact but without achieving a parallel cofacial configuration along the longitudinal axes. That is, the geometry that favours crystallisation and formation of weakly emissive interchain species such as aggregates or excimers. The term aggregate relates to species that have both the ground state and the emissive excited state delocalised among multiple chromophores while excimers are emissive excited-states shared between two or more chromophoric units with a dissociative ground state [26].

The emission spectra of **4a–d** in solution are qualitatively similar. Yet their film emission spectra show differences both in their emission spectral range and relative intensity of the vibronic bands. Thus, the film emission spectra of the low molecular weight **4a** have a red-shifted maximum and a large emission tail. Presumably, the larger number of chromophores near the chain ends in these short oligomers promotes the interaction between them in the solid state. In contrast, in dilute solution where chain interactions are strongly reduced the plain PL spectrum of **4a** represents emission from excited single chromophores. Therefore, at first glance the broad PL spectrum of **4a** could be due to emission from single chromophore and interchain species. Indeed, in a series of poly(*p*-dialkoxyphenylene)s which are structurally related to our terphenylene chromophore only short oligomers with $\text{DP} = 2\text{--}3$

Table 2
Solvent effects on emission maxima and lifetimes of **4a** and **4d**

	Solvent	Dilute conditions			Concentrated conditions		
		[c] ^a	$\lambda_{\text{PL, max}}$	τ^b	[c] ^a	$\lambda_{\text{PL, max}}$	τ^c
4a	Cyclohexane	Saturated ^d	374	–	–	–	–
	Ethyl acetate	3×10^{-3}	378	1.45 ± 0.03	1.0	380	1.33 ± 0.01
	THF	1×10^{-3}	376	–	1.0	383	–
	THF	2×10^{-2}	378	1.54 ± 0.01	5.0	411	1.30 ± 0.02
	Chloroform	2×10^{-2}	379	–	5.0	386	–
4d	Cyclohexane	Saturated ^d	375	–	–	–	–
	THF	1×10^{-3}	377	1.32 ± 0.01	1.0	373	1.58 ± 0.01
	Chloroform	2×10^{-2}	375	–	5.0	378	–

^a Concentration in mg/ml.

^b Observed lifetime at $\lambda_{\text{PL}} = 390$ nm, in ns.

^c Observed lifetime at $\lambda_{\text{PL}} = 420$ nm, in ns.

^d Samples were barely soluble, a saturated but highly dilute solution of unknown concentration was used.

showed a 460 nm band that was assigned to excimer emissions while longer chains showed a single emission maximum at 390 nm, presumably due to steric restrictions to form a cofacial configuration [27]. Similarly, we observed that the peculiar behaviour of **4a** in films is much reduced in the samples with higher degree of polymerisation. In particular, the neat film of **4d** gives a emission band centred at ca. 381 nm with weak vibronic coupling, a very small red shift of 4 nm as compared to the spectrum recorded in dilute solution and quite narrow full width at half-maximum, fwhm_{PL} . Thus, as the DP of the samples increases the fwhm_{PL} of film emissions decreases from 156 nm in **4a** to 64 nm in **4d** towards a limiting value, i.e., the 57 nm fwhm_{PL} of dilute solution emissions of **4a–d**. Notably, it also shows only a modest band broadening. Therefore, unlike previous studies that found aggregate species in films in others polymers, either fully conjugated [25,28] or segmented [5,6], there is no additional weak absorption band, red-shifted relative to that of a single chromophore, nor obviously red-shifted emission to immediately point to aggregate or excimer formation in either CHCl_3 solutions or, even more significant, in films of **4b–c**.

Moreover, a film of 1% **4a** in a PMMA matrix shows an emission spectra (Fig. 4a) similar to solution, thus indicating that intrachain folding do not originate the long wavelength bands and confirming that defect-driven energy transfer is not significant in either liquid or solid solutions of **4a**.

However, the presence of small amounts of aggregates cannot easily be ruled out because the tail of the absorption spectrum of the single chro-

mophore can blur its distinct absorption band. In bad solvents the PL spectrum of conjugated polymers like MEH-PPV usually shifts to red, the spectral shape changes and the decay dynamics become non-single exponential. These features are highly dependent on both solvent and concentration and are usually assigned to aggregate formation. Therefore, we carried out steady-state and time-resolved PL measurements for **4a** and **4d** in dilute and concentrated solutions of poorer solvents than CHCl_3 . Table 2 shows the solvatochromic and concentration effects on the PL of the extremes of this polymer series, **4a** and **4d**. In dilute solution no solvatochromism was observed in either **4a** or **4d**, only the weak vibronic structure of **4d** observed in CHCl_3 was lost in poorer solvents. Their luminescence decays, measured near the emission maxima at $\lambda_{\text{max}} = 390$ nm, were in every case monoexponential with a lifetime range of 1.4 ± 0.1 ns, a value close to the *p*-terphenylene radiative lifetime of 1 ns. Concentrated solutions of **4a** showed a somewhat different behaviour. Again, no solvatochromism was noted but instead their PL maxima are red shifted and present a moderate concentration dependence (Fig. 5a), though the PL decayed single exponentially with dilute-like solution lifetime values of 1.3 ns. These measurements at high concentration were made at $\lambda_{\text{max}} = 420$ nm in order to sample luminescence emitted from the red tail. Another attempt to detect non-single exponential decays was done on a highly concentrated THF solution of **4a**, which showed a PL spectrum resembling that of the film. Thus, as shown in Fig. 5a lifetimes were measured in the 380–480 nm range, i.e., including the red tail

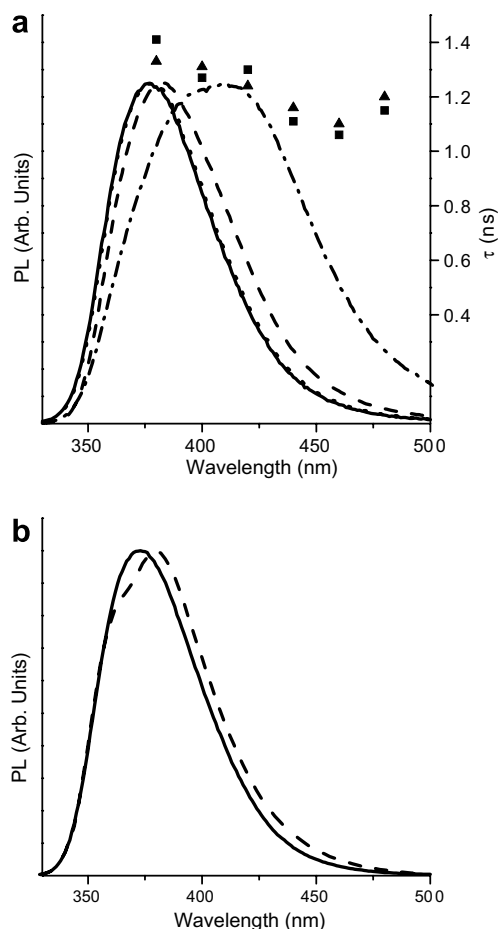


Fig. 5. (a) Normalized PL spectra of 1×10^{-3} (solid), 2×10^{-2} (dot), 1.0 (dash) and 5.0 (dot–dash) mg/ml solutions of **4a** in THF excited at 310 nm. Lifetimes (τ) of emission of **4a** measured with band-pass filter UG1 (■) and UG11 (▲). (b) Normalized PL spectra of 5 mg/ml solutions of **4d** in THF (solid) and CHCl_3 (dash) excited at 310 nm.

region, where supposedly aggregate contribution to luminescence would be maximised. Once more, all decays were monoexponential. Fig. 5b shows the emission spectra of **4d** in concentrated solutions of THF and CHCl_3 , as expected, the higher molecular weight **4d** showed similar behaviour in dilute and concentrated solutions. Consequently, all emissions registered should be assigned to the decay of single chromophore excitons including those from the **4a** tail. Therefore, lifetime measurements gave no evidence of the presence of sizeable amounts of long-lived species as aggregates or excimers; but since they are weakly emitting their presence could be difficult to detect (see Fig. 6).

In summary, we observed that both solution and film absorption spectra of **4a–d** are identical. Simi-

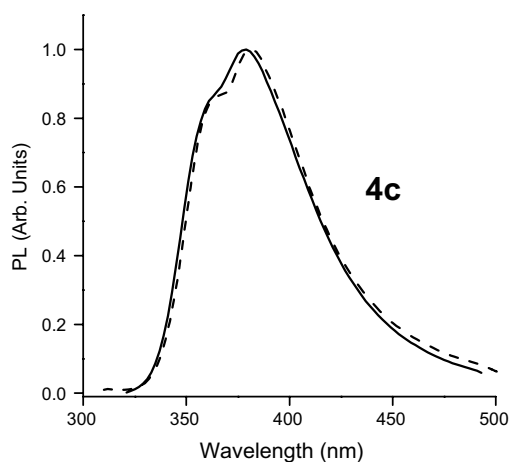


Fig. 6. Normalized emission spectra of **4c** before (solid) and after (dot) annealing at 190 °C for 6 h.

larly, the solution PL spectra of **4a–d** are equivalent. Neat films of **4b–d** show alike PL spectra that are slightly red-shifted compared to the solution PL spectra while only **4a** films showed emission that in principle could be attributed to interchromophore species but lifetime measurements do not support this point. However, it is worth noting that it could be difficult to pinpoint the nature of the structure responsible for the long wavelength emissions in conjugated systems and frequently, different studies ascribed variously the origin of these long wavelength emissions to either aggregates, excimers, oxidative defects or a combination of these species [29]. We also examined the effect of annealing on the film morphology and photoluminescence. Usually, long-term [30,31] or even short-term [32] thermal treatments of conjugated polymer films enhance interactions between vicinal chromophores that lead to noticeable red-shifted emissions from interchain species. However, the film PL spectra of either **4c** or **4d** recorded on the same samples before and after thermal annealing up to 6 h in a nitrogen atmosphere at 10 °C above their T_g values were identical, without showing any band broadening or decrease in fluorescence intensity. Therefore, the amorphous morphology of **4** proved to be very stable under thermal stress.

4. Conclusions

A new regularly segmented conjugated polymer was synthesized through Suzuki cross-coupling. The small size of the connector and lack of long lateral chains lead to a high density of rigid electrooptically

active moieties in the structure. However, the bent microstructure produces a highly soluble amorphous polymer with relatively high T_g . Its contorted chain conformation substantially hinders interactions between chromophores, thus diminishing to a great extent the formation of the aggregated species commonly observed in other electrooptically active polymers. Moreover, their absorption and emission properties are rather insensitive to Mn after reaching a modest DP, to the aggregation state, either solution or neat film, and to thermal stress. These properties could be of practical significance in view of the sensitivity of conjugated polymer morphology to polymer molecular weight, solvent nature, polymer concentration, ageing or heating of polymer solution, drop-cast or spin casting conditions, oxidation damage and thermal history. In addition, the high solubility of the polymer might allow incorporating larger aromatic units such as fluorene or pyrene while processability is retained. In fact, we already prepared a highly soluble homologous polymer with quaterphenylene units whose electrooptical properties are being evaluated [33].

Acknowledgements

Financial support was provided in parts by CONICET, ANPCyT and SGCyT-UNS. DR PG and A MF thank CONICET for fellowships.

References

- [1] Halls JJM, Arias AC, MacKenzie JD, Wu W, Inbasekaran M, Woo ED, et al. *Adv Mater* 2000;12:498.
- [2] (a) Schwartz BJ. *Ann Rev Phys Chem* 2003;54:141; (b) Campoy-Quiles M, Etchegoin PG, Bradley DDC. *Phys Rev B* 2005;72:45209; (c) Verlhac J-M, LeBlévenec G, Djurado D, Rieutord F, Chouiki M, Travers J-P, et al. *Synt Met* 2006;156:815.
- [3] Wood P, Samuel IDW, Webster GR, Burn PL. *Synt Met* 2001;119:571.
- [4] Shirota Y. *J Mater Chem* 2005;15:75.
- [5] Keegstra MA, Cimrová V, Neher D, Scherf U. *Macromol Chem Phys* 1996;197:2511.
- [6] Xia C, Advincula RC. *Macromolecules* 2001;34:6922.
- [7] Konstandakopoulou FD, Ionomopoulou SM, Gravalos KG, Kallitsis JK. *Chem Mater* 2000;12:2957.
- [8] Garcia Martinez A, Osio Barcina J, Fresno Cerezo A, Schlüter A-D, Fran J. *Adv Mater* 1999;11:27.
- [9] Faber R, Stasko A, Nuyken O. *Macromol Chem Rapid Commun* 2000;201:2257.
- [10] Ranger M, Rondeau D, Leclerc M. *Macromolecules* 1997;30:7686.
- [11] Sunagawa M, Matsumara H, Kitamara Y, European Patent 1991;0493032A2. Sumimoto Pharmaceuticals Company.
- [12] Wang C, Kilitziraki M, MacBride JAH, Brice MR, Horsburgh LE, Sheridan AK, et al. *Adv Mater* 2000;12: 217.
- [13] Steiger D, Tervoort T, Weder C, Smith P. *Macromol Rapid Commun* 2000;21:405.
- [14] Greiner A, Mang S, Schäfer O, Simon P. *Acta Polym* 1997; 48:1.
- [15] Brink-Spalink F, Greiner A. *Macromolecules* 2002;35:3315.
- [16] Beinhoff M, Bozano LD, Campbell Scott J, Carter KR. *Macromolecules* 2005;38:4147.
- [17] Clärner C, Greiner A. *Macromol Rapid Commun* 1998; 19:605.
- [18] Havelka-Rivard PA, Nagai K, Freeman BD, Sheares VV. *Macromolecules* 1999;32:6418.
- [19] Lakowicz JR. *Principles of Fluorescence Spectroscopy*. New York: Kluwer Academic/Plenum; 1999.
- [20] Gierschner J, Mack HG, Egelhaaf S, Schweizer S, Doser B, Oelkrug D. *Synt Met* 2003;138:311.
- [21] Matsuoka S, Fujii H, Yamada T. *J Phys Chem* 1991;95: 5802.
- [22] Gierschner J, Mack HG, Luer L, Oelkrug D. *J Chem Phys* 2002;116:8596.
- [23] DiCesare N, Belletête M, Rivera Garcia E, Leclerc M, Durocher G. *J Phys Chem A* 1999;103:3864.
- [24] Grell M, Bradley DDC, Long X, Chamberlain T, Inbasekaran M, Woo EM, et al. *Acta Polym* 1998;49:439.
- [25] Liao J-H, Benz M, LeGoff E, Kanatzidis MG. *Adv Mater* 1994;6:135.
- [26] Samuel IDW, Rumbles G, Friend RH. In: Sariciftci NS, editor. *Primary photoexcitations in conjugated polymers*. London: World Scientific Publishing Co. Pvt. Ltd.; 1997. p. 140–69.
- [27] Výprachtický D, Cimrová V, Machová L, Pokorná V. *Collect Czech Chem Commun* 2001;66:1473.
- [28] Mikroyannidis JA. *Synth Met* 2005;155:125.
- [29] (a) Sims M, Bradley DDC, Ariu M, Koeberg M, Asimakis A, Grell M, et al. *Adv Funct Mat* 2004;14:765; (b) Zhao W, Cao T, White JM. *Adv Funct Mat* 2004;14: 783.
- [30] Cho BJ, Son KH, Lee SH, Song Y-S, Lee Y-K, Jeon S-J, et al. *J Am Chem Soc* 2001;123:10039.
- [31] Schaller RD, Snee PT, Johnson JC, Lee LF, Wilson KR, Haber LH, et al. *J Chem Phys* 2002;117:6688.
- [32] Cho H-J, Jung B-J, Cho NS, Lee J, Shim H-K. *Macromolecules* 2003;36:6704.
- [33] Del Rosso PG, Almassio MF, Garay RO, to be published.